

# Multistrand RNA Secondary Structure Prediction and Nanostructure Design Including Pseudoknots

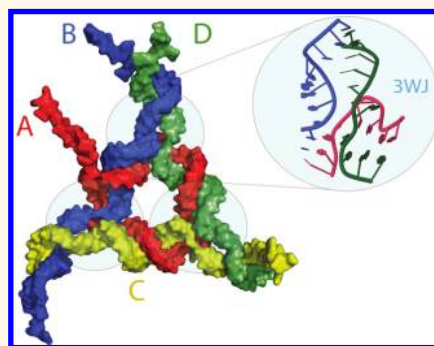
Eckart Bindewald,<sup>†</sup> Kirill Afonin,<sup>‡</sup> Luc Jaeger,<sup>§,⊥</sup> and Bruce A. Shapiro<sup>\*,\*</sup>

<sup>†</sup>Basic Science Program, SAIC-Frederick, Inc., NCI-Frederick, Frederick, Maryland, United States, <sup>‡</sup>Center for Cancer Research Nanobiology Program, NCI-Frederick, Frederick, Maryland, United States, <sup>§</sup>Department of Chemistry and Biochemistry, University of California, Santa Barbara, California 93106-9510, United States, and <sup>⊥</sup>Biomolecular Science and Engineering Program, University of California, Santa Barbara, California 93106-9510, United States

RNA is an attractive molecule class for the design of nanoscale structures that potentially possess multiple biochemical functions. RNA-based molecular complexes have been designed to form shapes resembling squares,<sup>1–4</sup> cubes,<sup>5,6</sup> an antiprism,<sup>7</sup> multimeric rings,<sup>8–10</sup> and a tri-star.<sup>11</sup> It is highly desirable to have computational tools that aid the structure prediction and design of such multistrand RNA complexes. The secondary structure prediction problem considered here is to computationally predict the base pairing of one or several RNA strands such that the predicted structure coincides with the experimentally determined base pairing. We are particularly interested in developing a computational method for the fast and accurate prediction of multistrand RNA nanostructures (tectoRNA).<sup>1,12,13</sup>

An example of a multistrand RNA secondary structure is shown in Figure 1. In a circular diagram (Figure 1, right) sequences are laid out in a clockwise direction along the circumference of the circle: base pairs or helices are represented as arcs; non-nested base pairs correspond to “crossing arcs”. We also call RNA secondary structures with non-nested base pairs pseudoknotted. The computational prediction of RNA secondary structures is greatly simplified if RNA secondary structures are assumed to consist of only base pairs that are nested. In this case it is possible to find the minimum free energy (MFE) structure with the help of recursion relationships that can be computationally solved with the use of dynamic programming algorithms.<sup>14–16</sup> Much of the recent work in this field has focused on considering subclasses of pseudoknots such that the minimum free energy structure can be found efficiently.<sup>17–19</sup> On the other hand, it has been mathematically proven that

## ABSTRACT



We are presenting NanoFolder, a method for the prediction of the base pairing of potentially pseudoknotted multistrand RNA nanostructures. We show that the method outperforms several other structure prediction methods when applied to RNA complexes with non-nested base pairs. We extended this secondary structure prediction capability to allow RNA sequence design. Using native PAGE, we experimentally confirm that four *in silico* designed RNA strands corresponding to a triangular RNA structure form the expected stable complex.

**KEYWORDS:** pseudoknot · RNA · secondary structure prediction · sequence design · tectoRNA

finding the minimum free energy RNA structure among the set of all (including non-nested) RNA secondary structures is equivalent to a class of problems for which no algorithm with polynomial complexity has yet been found.<sup>20,21</sup> For this case of unrestricted pseudoknot complexity, it will be desirable to develop heuristic algorithms (such as the one described in this paper) for the “search component” of RNA secondary structure prediction methods that are computationally efficient with the drawback that the solutions are not guaranteed to correspond to the minimum free energy structure.

Most current RNA secondary structure prediction methods use a physics-based energy model that is derived from a nearest-neighbor base pair stacking model.<sup>16,22,23</sup>

\* Address correspondence to shapirbr@mail.nih.gov.

Received for review July 15, 2011 and accepted November 8, 2011.

Published online November 08, 2011  
10.1021/nn202666w

© 2011 American Chemical Society

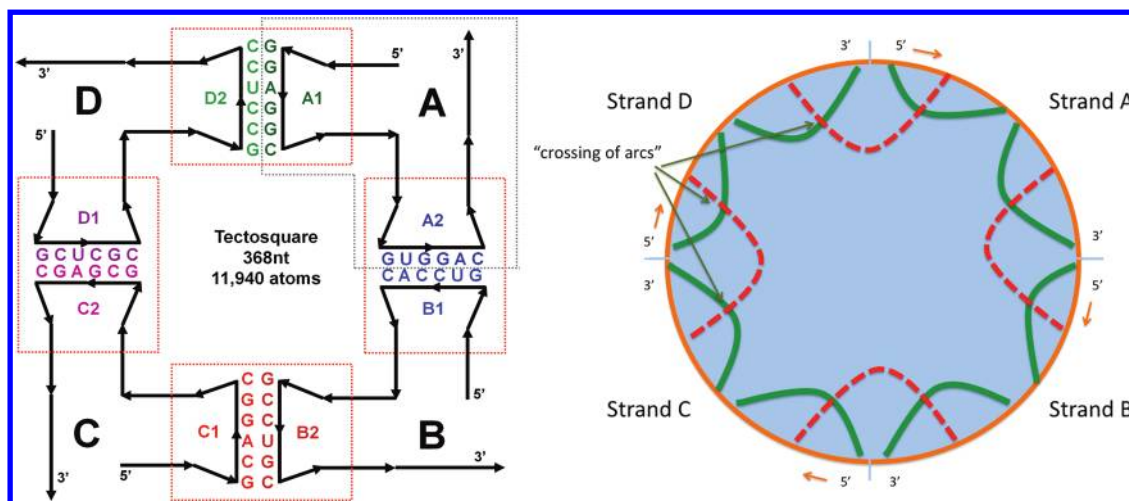


Figure 1. The internal representation of multistrand secondary structures corresponds to non-nested base pairings. Left: schematic of one of the four-strand RNA square designs (also called tectosquare).<sup>1</sup> Right: Equivalent circular plot of the computer-internal representation of the RNA square. Helices are represented as arcs. Non-nested base pairs correspond to crossing of arcs. A more detailed version of the circular representation of the RNA square is part of the screenshot shown in Figure 5. The left part of the figure has been reprinted from *Methods*, 54(2), Kasprzak *et al.*: Use of RNA structure flexibility data in nanostructure modeling, pp 239–250, copyright 2011, with permission from Elsevier.<sup>43</sup>

Machine-learning techniques have, however, also been applied successfully to single-strand RNA secondary structure prediction as well as to the problem of predicting RNA secondary structure from a set of aligned homologous sequences.<sup>24–26</sup>

Methods for predicting the intra- and interstrand base pairing of not more than two RNA strands are available in the form of the RNAfold program and the Pairfold program.<sup>27,28</sup> Computational tools for the secondary structure prediction of three or more sequences were notably absent until recently. Programs that are able to predict secondary structures of multiple RNA sequences are Multifold and NUPACK.<sup>18,29</sup> The NUPACK software considers pseudoknots for single RNA strands (the search space consists of all secondary structures that can be decomposed into two pseudoknot-free structures). This pseudoknot prediction capability is, however, currently not available for the prediction of two or more RNA strands. The inherent problem with not considering pseudoknotted structures (structures with non-nested base pairs) is shown for the example of an RNA square (see Figure 1): the base pairing that corresponds to the correct secondary structure is highly non-nested. For dynamic programming algorithms that do not consider pseudoknots (or only a subclass of pseudoknots), this can lead to the situation that the native secondary structure is not part of the search space and cannot be identified. This is the key motivation for the work presented here: the NanoFolder approach uses a very simple energy model, but has no restrictions on pseudoknot complexity.

The ability to predict RNA base pairing from a given sequence prompts the problem of sequence design: given a desired RNA base pairing, what should the sequence of the RNA strands be? Several programs

have been described that generate a novel sequence for a given pseudoknot-free single-strand RNA secondary structure. The RNAinverse program uses a Monte Carlo search in sequence space combined with dynamic programming that takes advantage of the fact that for a mutated sequence many energy terms from the previous sequence have not changed.<sup>16</sup> RNA-SSD performs a stochastic local search of near-optimal substructures in order to find a sequence whose predicted secondary structure matches the target secondary structure as close as possible.<sup>30,31</sup> Busch and Backofen described the program INFO-RNA.<sup>32,33</sup> It uses dynamic programming to generate an initial sequence. The initial sequence is further optimized with a local stochastic search using structural decomposition for fast energy computation and a look-ahead for the determination of favorable next mutation steps. The NUPACK package performs sequence optimization by minimizing the ensemble defect (the ensemble-averaged number of incorrectly paired nucleotides of the RNA or DNA complex).<sup>18,34</sup>

This paper is organized as follows: First, our approaches for the prediction as well as the design of pseudoknotted, multistrand RNA complexes are presented. We then evaluate the performance of the structure prediction approach using a test set of published RNA complexes. To demonstrate the viability of the RNA design approach, we lay out the steps involved in the design of a four-strand RNA triangular structure. Using native PAGE, we then verify experimentally that the *in silico*-designed RNA sequences form the desired complex.

## RESULTS

**Quality of Structure Prediction.** We used several published RNA structures that consist of three or more

strands as a test set to evaluate the quality of the RNA secondary structure predictions generated by NanoFolder. As a measure of how well the reference  $n \times n$  base pair matrix is predicted (with  $n$  being the total number of residues in the RNA strands) we use the Matthews correlation coefficient (Materials and Methods). Note that MCC values can range between 1 and  $-1$ . An MCC of 1 corresponds to a “perfect prediction” (*i.e.*, the predicted outcomes (base pairs) coincide with the correct result); an MCC of 0 corresponds to a random prediction with no correlation between prediction and the correct solution.

In Figure 2 we plot the Matthews correlation coefficient, comparing the programs NanoFolder and NUPACK. As one can see in the box-whisker plot, the median Matthews correlation coefficient (MCC) of the NanoFolder predictions is higher compared to NUPACK.

We also analyzed the performance of the program using a data set of 18 RNA heteroduplexes. We compared the prediction quality of the programs NanoFolder, NUPACK (program pairs), RNAcofold, and Pairfold.<sup>18,27,28</sup> Figure 3 shows a box-whisker plot of the

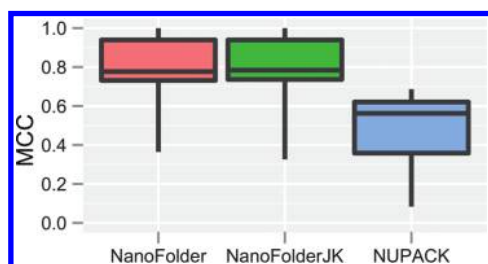


**Figure 2.** Box-whisker plot of achieved prediction qualities (Matthews correlation coefficients) for different methods applied to the set consisting of the nine multistrand RNA structures listed in Table 1. Each box-whisker element depicts the first quartile, median, and third quartile in the form of a colored box; minimum and maximum scores are depicted as “whiskers” (vertical lines emanating from the colored box element). No data elements were considered “outliers”. The method NanoFolderJK corresponds to the leave-one-out (jack-knife) approach of training and testing the interstrand interaction penalty parameter. For the method indicated as NanoFolder, this parameter was set to the median of the training results achieved in the jack-knife method.

different approaches. Results for RNAs corresponding to the eight non-nested secondary structures are shown on the left; results for RNAs corresponding to the 10 nested secondary structures are shown on the right. One can see that for non-nested RNA duplexes NanoFolder has the highest median prediction quality (MCC) compared to the other approaches; for RNA duplexes with nested base pairings (essentially helices possibly containing bulges and internal loops) the median prediction quality of NanoFolder is lower compared to the other approaches.

The run times of the NanoFolder program are shown in Table 1. The RNA square (368 residues) is computed in about 0.4 s; the RNA antiprism complex with 1008 residues is computed in less than 3 s. This suggests that the structure prediction algorithm is sufficiently fast to be useful in many practical situations.

**TABLE 1.** Prediction Results for RNA Structures with Three or More Strands<sup>a</sup>

name	ref	strands	residues	NanoFolderJK	NanoFolder	pairs	time (s)
hairpin riboz. (2P7F)	44	4	60	0.82	0.82	0.56	0.053
nanosquare (3P59)	2	4	100	0.40	0.36	0.08	0.052
antiprism (lower half)	6	4	504	0.74	0.75	0.69	0.617
antiprism (upper half)	6	4	504	0.78	0.73	0.62	0.654
RNA square	1	4	368	0.97	0.97	0.36	0.425
hexameric ring	8	6	264	0.33	0.63	0.10	0.199
antiprism	6	8	1008	0.78	0.78	0.63	2.913
six-stranded cube	4	6	288	1.00	1.00	0.53	0.233
10-stranded cube	4	10	332	0.94	0.94	0.57	0.252

<sup>a</sup> Strands: number of input RNA sequences; ref: literature reference; residues: total number of nucleotides; NanoFolderJK: NanoFolder results (Matthews correlation coefficient, MCC) using jack-knifing (such that current structure was not used during training); pairs results (MCC) from the NUPACK pairs program; NanoFolder: results (MCC) of NanoFolder using standard parameters. Time: run-time of the NanoFolder program (in seconds), evaluated using a Linux PC with a 3.0 GHz Intel Xeon processor.

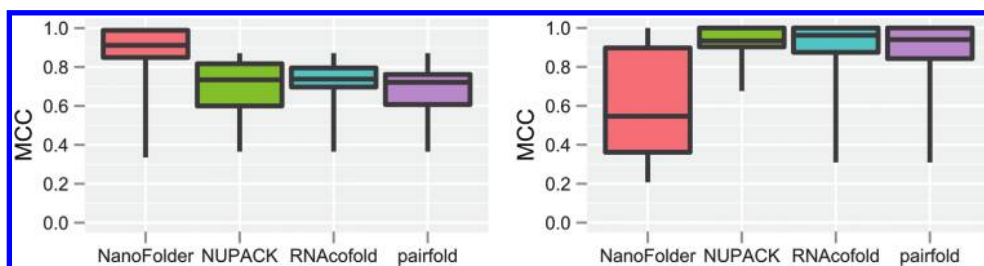


**Figure 3.** Box-whisker plot of achieved prediction qualities (Matthews correlation coefficients) for different methods applied to a test set consisting of 18 RNA heteroduplexes (Materials and Methods). Each box-whisker element depicts the first quartile, median, and third quartile in the form of a colored box; minimum and maximum scores are depicted as “whiskers” (vertical lines emanating from the colored box element). No data elements were considered “outliers”. Left: accuracies of structure predictions corresponding to a data set of duplex structures with non-nested base pairs. Right: accuracies of structure predictions corresponding to a data set of duplex structures not containing non-nested base pairs.

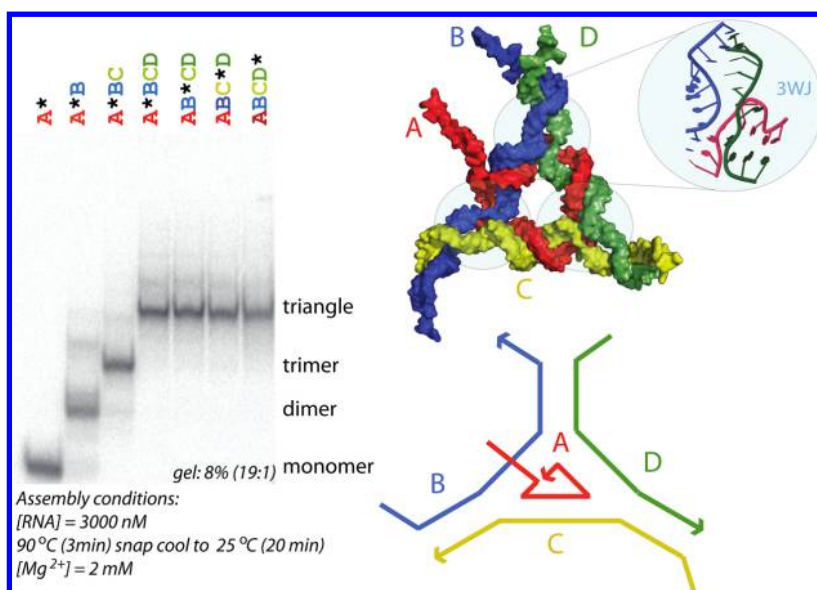


**Figure 4.** Right: molecular model of four-strand triangular RNA nanoscale structure. Shown is also the three-way junction that was obtained from the RNAJunction database (RNAJunction database accession ID 11836). Each of the 3 “corners” of the designed triangular structure contains this three-way junction(3WJ)motif. Left: Native PAGE results for different strand combinations.

To demonstrate the utility of the design approach, we designed *de novo* an RNA nanoscale structure that forms a triangular shape and consists of four RNA strands (see Figure 4, top right and bottom right). The three corners of the triangular structure are formed by one type of three-way junction motif that was identified with the help of the RNAJunction database and the NanoTiler software.<sup>35,36</sup> The sequence segments corresponding to the corner motif as well as the 5' ends were not modified during the sequence optimization; those residues are indicated in lower case in the sequences reported in the Materials and Methods section.

The formation of a four-strand RNA complex was experimentally verified using non-denaturing polyacrylamide gel electrophoresis (native-PAGE). This electrophoretic separation technique is widely used for characterizations of RNA assemblies (Afonin, *et al. Nat. Protoc.* **2011**). Major dark bands on the gel correspond to the products of the assemblies (see Figure 4, left). Assembled four-strand RNA complexes are expected to migrate as a single band with the lowest mobility. Native-PAGE results presented in Figure 4 demonstrate the reproducible self-assembly of four (A–D) RNA strands, into the definite structure of a tetramer. Quantification of the bands reveals that the average yield of the RNA tetramer is greater than 90%. To verify that all four RNA strands participate in self-assembly, each of the four radiolabeled molecules (marked with “\*”) was individually mixed with three other nonlabeled molecules followed by the assembly protocol described in the Methods section. The results show identical gel shifts for all four tetramers with different labeled strands, suggesting the participation of all strands in the formation of the closed species.

**Web Server.** We implemented a publically available Web server in order to provide a user-friendly interface for the structure prediction and sequence design methodology. Input for the secondary structure prediction is a set of RNA sequences in FASTA format. Figure 5 shows a screenshot of a secondary structure prediction result that one obtains after submitting four RNA sequences that correspond to the RNA square.<sup>1</sup> The predicted base pairing is shown on the result page in three different text formats as well as an image depicting a circular diagram.

Input to the sequence design method is a set of RNA sequences combined with a descriptor for the desired target secondary structure (input format examples are given on the Web page). Nucleotides that are represented as uppercase (lowercase) characters in the user-defined starting sequences will (not) be modified during sequence randomization and optimization, respectively. This effectively makes possible partial sequence optimization that can be useful for optimizing a set of sequence in stages as well as for keeping structural motifs unchanged. The user also can specify the number of iterations corresponding to the two stages of optimization. The URL of the Web server is <http://matchfold.abcc.ncifcrf.gov/>.

## DISCUSSION

The secondary structure prediction algorithm of NanoFolder is strikingly simple: it proceeds by placing in a “greedy” fashion RNA helices in the order of their estimated free energy. This approach has the advantage that it is fast and that it is unrestricted in terms of pseudoknot complexity. Indeed, to the best of our knowledge, NanoFolder is currently the only computational



method that considers non-nested base pairings for multistrand secondary structure predictions. The computational multistrand predictions rely on the step of appending the multiple strands in a linear fashion, keeping track of the discontinuities between sequences.<sup>18,27,29</sup> A circular representation reveals that this procedure effectively turns the multistrand structure prediction problem into a single-sequence structure prediction problem with pseudoknots (see Figures 1 and 5). Only allowing a subclass of pseudoknots or not allowing pseudoknots at all potentially prohibits the target secondary structure from being part of the solution set. A sequence design algorithm with that restriction will then have to rely on a structure prediction methodology that considers only partially folded or misfolded structures.

The relative importance of considering pseudoknots *versus* the sophistication of the energy model becomes particularly apparent when considering the structure prediction results shown in Figure 3. The plot depicts structure prediction results of the various approaches (NanoFolder, NUPACK, RNAfold, Pairfold) to a set of RNA heteroduplexes. When applied to a data set of RNA duplexes with non-nested base pairs (Figure 3 left), NanoFolder outperforms the other methods, even though its energy model is much simpler. When applied to the data set of RNA duplexes not containing non-nested base pairs (Figure 3 right), NanoFolder predictions are less accurate compared to the other

methods. This is likely due to the simple energy model (essentially consisting of only two terms) employed by NanoFolder. Also apparent from Figure 3 is that the structure prediction results of the three programs NUPACK, RNAfold, and Pairfold are similar in quality. This is likely due to the similarity in the search algorithms (dynamic programming) and energy models. It would be desirable to develop a multistrand RNA secondary structure prediction algorithm that is based on the energy model of the aforementioned programs and yet has no restriction in terms of pseudoknot complexity.

This also suggests that designed architectonic RNAs possess different properties compared to natural RNAs. The key for tectoRNAs is robustness of folding (often implemented by using relatively long helices). Indeed, in the field of DNA nanoscale structure design, impressively complex DNA structures have been designed and experimentally verified using a set of heuristic rules without ever attempting a full minimum free energy DNA secondary structure prediction.

The NanoFolder design algorithm is specifically geared toward the design of tectoRNAs. It is a combination of RNA secondary structure prediction and sequence design rules. The demonstrated high secondary structure prediction accuracy combined with the shown experimental (native PAGE) confirmation of a designed RNA triangular structure makes us confident that NanoFolder is an important addition to the toolkit of an RNA nanostructure designer.

## MATERIALS AND METHODS

**RNA Structure Data Sets.** We developed two data sets for training and testing the multistrand RNA secondary structure prediction algorithm. Eighteen RNA structures consisting of two RNA strands with nonidentical sequences (heteroduplexes) were obtained from the PDB databank. Their PDB accession codes are for nested structures 1NTA, 2D1A, 2G5K, 2OE5, 2OEU, 2PN3, 2XEB, 3BNP, 3CJZ, and 429D; for non-nested structures the accession codes are 1BJ2, 1F27, 1YKQ, 2GCS, 2JLT, 2P89, 2PCW, and 3MJ3. We call this data set the heteroduplex set. Another data set (called the multistrand data set) consisting of nine RNA structures (each possessing three or more RNA strands) was generated using the Protein Data Bank as well as the available literature. These structures and their literature references are listed in Table 1.

**Multistrand Structure Prediction Including Pseudoknots.** A new program called NanoFolder performs the multistrand RNA secondary structure prediction. The main characteristics of the implementation are fast execution times as well as no restriction in terms of pseudoknot complexity. The RNA secondary structure scoring function and the search algorithm used by NanoFolder are described below.

**Scoring of RNA Structures.** The free energy contribution of an RNA double-helix is estimated using the sum of its base-pair stacking energies from a standard nearest neighbor energy model<sup>22</sup> as well as an interstrand penalty term that is zero for intrastrand helices and greater than zero for interstrand helices. Instead of using a physical model with parameters that are unknown or hard to measure, the value of the interstrand penalty term is determined using a training set (the interstrand penalty can be viewed as an entropic penalty). Training has

been performed in a jack-knife manner using the results corresponding to the nine RNA structures reported in Table 1. In other words, for each predicted RNA structure, the trained value of the interstrand penalty has been determined using the remaining eight RNA structures. For a given "test RNA", the search for the optimal interstrand penalty was an exhaustive enumeration of values between 0.0 and 2.0 kcal/mol in steps of 0.2 kcal/mol. The interstrand penalty that led to the highest prediction accuracy of the training set was then applied to the prediction of the one RNA of the test set. This procedure was repeated nine times, corresponding to the nine RNAs of the set shown in Table 1. The median of the nine chosen interstrand penalties was found to be 1.0 kcal/mol. This approach should be viewed as an empirical scoring function for RNA complexes rather than a physical energy function.

**RNA Folding Algorithm.** The structure prediction algorithm proceeds as follows: first, an exhaustive list of all possible helices consisting of two or more base pairs is generated. Each helix is scored as described in the previous section. To predict an RNA secondary structure, an RNA is folded *in silico* by placing the helices in ascending order of their scores, such that a newly placed helix is not overlapping with previously placed helices. If several unplaced helices have the same score contribution, a random choice is made to place one of them. The algorithm terminates when there are no helices in the original helix list that have not been placed yet and that do not overlap with already placed helices.

**RNA Sequence Design Algorithm.** The sequence design algorithm has the task of generating a set of RNA sequences that fold into a secondary structure that is as close as possible to the folding pattern envisioned by the designer. In addition, there

are “rules” that the designed sequences should obey. This lays out the general strategy for sequence design: Given an initial set of RNA sequences, the sequences are computationally mutated. Each set of RNA strands is scored using an objective function, which reflects how “good” the current set of sequences is. Using a Monte Carlo algorithm, the mutations of the sequences are accepted or rejected using a Metropolis criterion that depends on the difference in the values of the objective function as a consequence of the current mutation. The objective function consists of two components: a secondary structure similarity component and a sequence design rule component. Both terms are described in more detail in the following two sections.

**Secondary Structure Similarity Component.** This score component reflects the similarity of the predicted multistrand secondary structure and the desired target secondary structure. For the design of thermodynamically stable scaffold sequences, one wants the designed sequences to exhibit “robust” RNA folding. One can express this concept using an  $n \times n$  matrix (with  $n$  being the total number of residues in all RNA strands) containing probabilities of base pairing between different residues. The desired secondary structure corresponds to a base pair probability matrix containing matrix elements that have a value of 1 for desired base pairs and a value of 0 for undesired base pairs. This idealized probability of base pairing is then compared to the predicted base pair probability matrix. The more similar the predicted base pair probability matrix is to the idealized base pair probability matrix, the better the sequence design.

The base pair probability matrix is computed as follows: For a set of multistrand RNA strands a secondary structure prediction is rerun 20 times, each time adding a Boltzmann-weighted noise term to the energy contribution of each helix that is part of the initial exhaustive list of all possible helices. This leads to a set of 20 predicted secondary structures. The average occupancy of each base pair is used to generate an estimated base pair probability matrix.

From the base pair probability matrix  $P$ , the reference secondary structure  $s$ , the total number of residues  $n$ , a similarity score  $d(P, s)$  is computed as follows:

$$d(P, s) = \sum_{i=1}^n d_i(P, s)$$

with

$$d_i(P, s) = \begin{cases} 1 - P(i, B(i, s)), & \text{if } S(i) = 1 \\ \sum_{j=1}^n P(i, j), & \text{if } S(i) = 0 \end{cases}$$

The function  $S(i)$  is defined to be 1 if reference residue  $i$  participates in any base pairing and 0 otherwise. The function  $B(i, s)$  is defined to be equal to the index of the residue that participates in base pairing with residue  $i$ .

**Sequence Design Rule Component.** This score component reflects how well the designed RNA sequences “obey” a set of sequence design rules. Several design rules can be formulated using the concept of same-length sequence fragments called “critons”: From a sequence of length  $N$  one can generate  $N - L + 1$  contiguous sequence fragments (critons) of length  $L$ . We choose the length  $L$  of the considered critons to be 6nt. Rules based on the concept of critons have been applied with great success to the design of DNA nanostructures.<sup>37,38</sup> Each “rule violation” is computationally modeled as a penalty term. For example, branch migration is a property that is usually not desired in designed nucleotide sequences, because it potentially leads to a variety of structurally and energetically similar folds. In order to bias designed RNA sequences to not exhibit branch migration, a branch migration penalty term is set equal to the number of RNA double-helix ends that might contribute to branch migration. A subset of the employed set of rules has previously been used for the design of cubic RNA complexes.<sup>4</sup>

Here we present a list of the employed penalty scoring terms for the sequence design: 1) auViolation—Let  $k$  be the number of helical AU regions (sequence regions that consist only of nucleotides A or U and correspond to nucleotides that are per design desired to participate in base pairing) with a

length of three or more nucleotides. The penalty term is defined as  $s_{\text{AU}} = \sum_{i=1}^k (l_i - 2)$  with  $l_i$  being the length of the  $i$ th such AU region. The rationale for this term is to avoid designed helices that possess regions with too many consecutive A-U base pairs, which could result in helical regions with limited stability. 2) branchMigration—Count of the number of helix ends in the target secondary structure that could participate in branch migration. Let  $i, j$  be the indices of two residues that are base-paired in the target structure. If residue pair  $i+1, j-1$  (or  $i+1, j-1$ ) is not part of the target secondary structure but is Watson–Crick complementary, the branch-migration counter is increased by one. The rationale for this term is to promote a unique native structure (being equal to the target design structure) without having energetically similar structures corresponding to migrated junctions or partially opened helices. 3) complement—Count of the number of critons for which a reverse-complement criton exists that is not desired to base pair according to the target structure. The key idea of “critons” is that each criton cannot form complete duplexes with any other criton forming base pairs that are not part of the target structure; 4) consecutive—Count of the number of adjacent G or non-G nucleotides of the same kind that exceed two or three, respectively. A large number of adjacent nucleotides of the same type is not desirable, because it can potentially lead to a large set of structurally and energetically similar RNA folds. 5) duplicate—Count of the number of nonunique critons. If we denote the total number of generated critons from the input sequence(s) as  $n_c$ , and the number of unique sequence fragments obtained from these critons as  $n_u$ , we can express the scoring term as equal to  $n_c - n_u$ . Developing nonredundant sequences is the central idea of nucleic acid sequence design and dates back to the work of Ned Seeman.<sup>38</sup> Duplicate critons can lead to ambiguities in the RNA folding process, potentially leading to a riboswitch-like structure; 6) gcFracViolation—If the target secondary structure consists of  $k$  helices, there are  $2k$  helical strands in the target structure. Let  $c_{\text{GCmin}}(i) = \lfloor f_{\text{GC}} l_i \rfloor$  be the minimum number of desired G or C bases in the  $i$ th helical strand ( $l_i$  indicates the length of the  $i$ th helical strand, the constant  $f_{\text{GC}}$  is set to 0.76, the square brackets indicate rounding to the nearest lower integer). Let  $c_{\text{GC}}(i)$  be the count of the number of G or C nucleotides in the  $i$ th helical strand. The score is defined as

$$s_{\text{GCfrac}} = \sum_{i=1}^{2k} \begin{cases} c_{\text{GCmin}}(i) - c_{\text{GC}}(i), & \text{if } c_{\text{GCmin}}(i) > c_{\text{GC}}(i) \\ 0 & \text{otherwise} \end{cases}$$

The rationale of this term is to promote a high G+C content in helices; 7) gcViolation—Let  $k$  be the number of helical GC regions (sequence regions that consist only of nucleotides G or C and correspond to nucleotides that are per design desired to participate in base pairing) with a length of two or more nucleotides. The penalty term is defined as  $s_{\text{GC}} = \sum_{i=1}^k (l_i - 1)$  with  $l_i$  being the length of the  $i$ th GC region. The rationale for this term is to avoid helical regions that correspond to a long stretch of only GC base pairs; 8) selfComplement—Count of the number of critons that are self-complementary. Self-complementary regions are not desirable because they can potentially lead to the formation of unwanted hairpin structures; 9) smallComplement—Count of the number of small critons (length 4) that cannot be matched with a reverse-complementary small criton. This term promotes the formation of some base pairing in order to avoid completely unstructured RNA strands. This is useful to allow slightly structured regions, which are presumably more stable compared to completely unfolded structures with regard to nuclease degradation; 10) zipper—Count of the number of non G-C base pairs at helix ends. The rationale for this term is to favor folded RNA structures whose helices are not “breathing” (temporarily partially unfolding) but are terminated by thermodynamically stable G-C base pairs.

The weights of the scoring terms have not been optimized; the weight of each scoring term is 1.0 with the exception of the smallComplement term. This term has a weight of 0.1 because it addresses a design goal (stability with respect to nuclease degradation) of lower priority.

**Sequence Optimization Algorithm.** The task of the sequence optimization algorithm is to identify a set of RNA sequences that

correspond to a low design penalty score. The algorithm consists of three stages:

In the first stage, the RNA sequences are randomized; that is, the nucleotides of the RNA sequences are randomly chosen. The randomization is performed such that nucleotides that are designed to form base pairs are Watson–Crick complementary. The probabilities of choosing the bases A, C, G, and U are 0.2, 0.3, 0.3, and 0.2, respectively, corresponding to a G+C content of 60%. It is possible to define constant sequence regions that are not modified by the sequence optimization algorithm. This computational stage is finished once the initial identity of all residues has been specified.

In the second stage, the sequences are iteratively modified using a Monte Carlo algorithm combined with a Metropolis criterion (this approach is also called stochastic tunneling).<sup>39</sup> Nucleotides that correspond to lowercase characters in the input sequence data are not modified during the optimization. The objective function of this optimization stage is the rule-based score component (the sum of the terms listed in the section Sequence design rule component). This computational stage is finished after a user-defined number of iterations (default: 10 000 iterations).

In the third stage, the set of RNA sequences are further optimized (using the same Monte Carlo algorithm) using as an objective function that is the sum of the rule-based score component and the secondary structure similarity component. This computational stage is finished after a user-defined number of iterations (default: 1000 iterations).

The user can set the number of iterations of the second and third stage. This three-stage approach of generating optimized

sequences is rerun five times, and the set of RNA sequences that corresponds to the lowest objective function score is returned as a result.

**Secondary Structure Prediction Programs Used for Comparison NUPACK.** The NUPACK program Pairs (part of NUPACK software version 3.0) was used with the option `–multi` for multi-strand secondary structure prediction.<sup>18</sup>

**RNAcofold.** The RNAcofold program (part of the Vienna package 1.7.2) was used with default parameters.<sup>27</sup>

**Pairfold.** The Pairfold program of the MultiRNAfold package (version 2.0) was used with default parameters.<sup>28</sup>

**Matthews Correlation Coefficient As a Measure of Prediction Quality.** The Matthews correlation coefficient is widely used to compare the performance of binary classifiers.<sup>40</sup> For a set of RNA strands (with a total number of  $n$  residues), a multistrand RNA secondary structure can be represented by a  $n \times n$  matrix (“base pair matrix”) that has matrix elements that are 1 for residues that are base-paired and 0 otherwise. To compute the MCC for a predicted secondary structure, we compute the base pair matrix corresponding to the predicted secondary structure and the reference secondary structure. Each element of the predicted base pair matrix corresponds to one of four cases, depending on whether it is a true positive, false positive, false negative, or true negative prediction. From the four numbers (true positives (TP), false positives (FP, the total number), true negative (TN), false negatives (FN)), the Matthews correlation coefficient is computed using the equation

$$\text{MCC} = \frac{\text{TP} \cdot \text{TN} - \text{FP} \cdot \text{FN}}{\sqrt{(\text{TP} + \text{FP})(\text{TP} + \text{FN})(\text{TN} + \text{FP})(\text{TN} + \text{FN})}}$$

## EXPERIMENTAL PROCEDURES

As described in the Results section, a triangular RNA structure consisting of four strands was experimentally tested for complex formation in order to test the viability of the sequence design approach. The experimental steps are described in detail in this section.

**RNA Preparation.** Synthetic DNA molecules coding for the antisense sequence of the designed RNA were purchased from IDT DNA and amplified by PCR using primers containing the T7 RNA polymerase promoter. PCR products were purified using the QiaQuick PCR purification kit, and RNA molecules were prepared enzymatically by *in vitro* transcription using T7 RNA polymerase. Samples were incubated at 37 °C for four hours in a buffer containing 15 mM MgCl<sub>2</sub>, 2 mM spermidine, 50 mM Tris buffer (pH 7.5), 2.5 mM NTPs, 10 mM DTT, 0.1 μg/μL IPP, and 0.8 u/μL RNasin; the reaction was quenched by adding 5 μL of RQ1 RNase-free DNase (10 u/μg) for a reaction volume of 200 μL, followed by 30 additional minutes of incubation. Samples were purified on a denaturing urea gel (PAGE) (8% or 10% acrylamide, 8 M urea). The RNA was eluted from gel slices overnight at 4 °C into buffer containing 300 mM NaCl, 10 mM Tris pH 7.5, and 0.5 mM EDTA. After precipitating the RNA in two volumes of 100% ethanol, samples were rinsed twice with 75% ethanol, vacuum-dried, and dissolved in TE buffer.<sup>41,42</sup>

**Co-transcriptional α[<sup>32</sup>P]-ATP Body Labeling of RNA Molecules.** DNA templates (containing the T7 RNA polymerase promoter) were added to the transcription mixture (diH<sub>2</sub>O, 50 mM Tris pH 7.5, 10 mM MgCl<sub>2</sub>, 2 mM spermidine, 2.5 mM NTPs, 10 mM DTT) containing α[<sup>32</sup>P]-ATP (10 mCi/mL) for body labeling. Transcription was initiated with the addition of T7 RNA polymerase and stopped after 4 h with RQ1 RNase-free DNase. Labeled material was purified as described above.

**Nondenaturing PAGE Experiments.** All assembly experiments reported in this study were analyzed on 8% (19:1) nondenaturing polyacrylamide native gels containing 2 mM Mg(OAc)<sub>2</sub> and 50 mM KCl and run at 4 °C with running buffer (89 mM Tris-borate, pH 8.3/15 or 2 mM Mg(OAc)<sub>2</sub>). Prior to the addition of the buffer and Mg(OAc)<sub>2</sub>, the RNA samples containing cognate RNA molecules at concentrations of 3 μM were heated to 90 °C for

3 min and immediately snap cooled at 25 °C followed by assembly buffer addition (tris-borate buffer (89 mM, pH 8.3), 2 mM Mg(OAc)<sub>2</sub>) and incubation for 20 min. An equal volume of loading buffer (same buffer with 0.01% bromophenol blue, 0.01% xylene cyanol, 50% glycerol) was added to each sample before loading on the native gel. Gels were run for 4 h, at 25 W with the temperature set to below 10 °C, dried under vacuum, exposed to a phosphorimager screen for 16 h, and scanned using a Storm 860 phosphorimager. Band quantification was performed using commercially available ImageQuant software. Equally sized boxes were drawn around the bands corresponding to the assembled RNA complexes. The yields of RNA complexes were calculated by dividing their corresponding quantified values by the total sum of the values for all other complexes present in the corresponding lane.

**RNA Sequences Used in This Example.** The RNA sequences used are listed below. Nucleotides that underwent sequence optimization are shown in upper case; the remaining nucleotides (shown in lower case) correspond to either the chosen three-way junction motif or the starting sequence motifs.

A: gggaaAUGACUCUcgucagGACACUCUCgucagCUCUGU  
GUGgucagAGUCG  
B: ggaaGUCACGGUCUcgacgacgAGAGCGACUcgcaaccACA  
CUGGUGAC  
C: ggaaCAGUGUgacgacgCACACAGAGcgcaaccCACUGC  
D: ggaaGCAGUGgacgacgGAGAGUGUCcgcaaccGAGACC

**Three-Way Junction Motif.** The three-way junction that is used for the triangular RNA structure (described in the Results section) was identified using the RNAjunction database, by searching for a three-way junction that contains an interhelix angle that is similar to 60° and two interhelix angles similar to 150°. This structural element (RNAjunction accession ID 11836) was extracted from the *Thermus thermophilus* 16S rRNA structure (PDB: 2J00). The triangular structure was identified using a combinatorial search performed with the NanoTiler software.<sup>36</sup>

**Acknowledgment.** We thank Wojciech Kasprzak as well as the ABCC computing center of the NCI-Frederick for the



computational support. This research was supported (in part) by the Intramural Research Program of the NIH, National Cancer Institute, Center for Cancer Research. This project has been funded in whole or in part with federal funds from the National Cancer Institute, National Institutes of Health, under contract HHSN261200800001E. The content of this publication does not necessarily reflect the views or policies of the Department of Health and Human Services, nor does mention of trade names, commercial products, or organizations imply endorsement by the U.S. government. This research was also supported by NIH grant R01 GM079604 (to L.J.).

## REFERENCES AND NOTES

- Chworos, A.; Severcan, I.; Koyfman, A. Y.; Weinkam, P.; Oroudjev, E.; Hansma, H. G.; Jaeger, L. Building Programmable Jigsaw Puzzles with RNA. *Science* **2004**, *306*, 2068–2072.
- Dibrov, S. M.; McLean, J.; Parsons, J.; Hermann, T. Self-Assembling RNA Square. *Proc. Natl. Acad. Sci. U. S. A.* **2011**, *108*, 6405–6408.
- Severcan, I.; Geary, C.; Verzemnieks, E.; Chworos, A.; Jaeger, L. Square-shaped RNA particles from different RNA folds. *Nano Lett.* **2009**, *9*, 1270–1277.
- Afonin, K. A.; Bindewald, E.; Yaghoubian, A. J.; Voss, N.; Jacovetty, E.; Shapiro, B. A.; Jaeger, L. In Vitro Assembly of Cubic RNA-Based Scaffolds Designed in Silico. *Nat. Nanotechnol.* **2010**, *5*, 676–682.
- Afonin, K. A.; Grabow, W. W.; Walker, F. M.; Bindewald, E.; Dobrovolskaia, M. A.; Shapiro, B. A.; Jaeger, L. Design and Self-Assembly of siRNA-Functionalized RNA Nanoparticles for Use in Automated Nanomedicine. *Nat. Protoc.* **2011**, *6* (in press).
- Severcan, I.; Geary, C.; Chworos, A.; Voss, N.; Jacovetty, E.; Jaeger, L. A Polyhedron Made of tRNAs. *Nat. Chem.* **2010**, *2*, 772–779.
- Chen, C.; Sheng, S.; Shao, Z.; Guo, P. A Dimer as a Building Block in Assembling RNA. A Hexamer That Gears Bacterial Virus Phi29 DNA-Translocating Machinery. *J. Biol. Chem.* **2000**, *275*, 17510–17516.
- Grabow, W. W.; Zakrevsky, P.; Afonin, K. A.; Chworos, A.; Shapiro, B. A.; Jaeger, L. Self-Assembling RNA Nanorings Based on RNAi/ii Inverse Kissing Complexes. *Nano Lett.* **2011**, *11*, 878–887.
- Yingling, Y. G.; Shapiro, B. A. Computational Design of an RNA Hexagonal Nanoring and an RNA Nanotube. *Nano Lett.* **2007**, *7*, 2328–2334.
- Geary, C.; Chworos, A.; Jaeger, L. Promoting RNA helical stacking via A-minor junctions. *Nucleic Acids Res.* **2011**, *39*, 1066–1080.
- Shu, D.; Shu, Y.; Haque, F.; Abdelmawla, S.; Guo, P. Thermodynamically Stable RNA Three-Way Junction for Constructing Multifunctional Nanoparticles for Delivery of Therapeutics. *Nat. Nanotechnol.* **2011**, *6*, 658–667.
- Jaeger, L.; Chworos, A. The Architectonics of Programmable RNA and DNA Nanostructures. *Curr. Opin. Struct. Biol.* **2006**, *16*, 531–543.
- Jaeger, L.; Westhof, E.; Leontis, N. B. TectoRNA: Modular Assembly Units for the Construction of RNA Nano-Objects. *Nucleic Acids Res.* **2001**, *29*, 455–463.
- Nussinov, R.; Pieczenik, G.; Griggs, J. R.; Kleitman, D. J. Algorithms for Loop Matchings. *SIAM J. Appl. Math.* **1978**, *35*, 68–82.
- Zuker, M.; Stiegler, P. Optimal Computer Folding of Large RNA Sequences Using Thermodynamics and Auxiliary Information. *Nucleic Acids Res.* **1981**, *9*, 133–148.
- Hofacker, I. L.; Fontana, W.; Stadler, P. F.; Bonhoeffer, S.; Tacker, M.; Schuster, P. Fast Folding and Comparison of RNA Secondary Structures. *Monatsh. Chem.* **1994**, *125*, 167–188.
- Reeder, J.; Steffen, P.; Giegerich, R. pknotsRG: RNA Pseudoknot Folding Including near-Optimal Structures and Sliding Windows. *Nucleic Acids Res.* **2007**, *35*, W320–324.
- Zadeh, J. N.; Steenberg, C. D.; Bois, J. S.; Wolfe, B. R.; Pierce, M. B.; Khan, A. R.; Dirks, R. M.; Pierce, N. A. NUPACK: Analysis and Design of Nucleic Acid Systems. *J. Comput. Chem.* **2010**, *32*, 170–173.
- Rivas, E.; Eddy, S. R. The Language of RNA: A Formal Grammar That Includes Pseudoknots. *Bioinformatics* **2000**, *16*, 334–340.
- Lyngso, R. B.; Pedersen, C. N. RNA Pseudoknot Prediction in Energy-Based Models. *J. Comput. Biol.* **2000**, *7*, 409–427.
- Akutsu, T. Dynamic Programming Algorithms for RNA Secondary Structure Prediction with Pseudoknots. *Discrete Appl. Math.* **2000**, *104*, 45–62.
- Mathews, D. H.; Sabina, J.; Zuker, M.; Turner, D. H. Expanded Sequence Dependence of Thermodynamic Parameters Improves Prediction of RNA Secondary Structure. *J. Mol. Biol.* **1999**, *288*, 911–940.
- Zuker, M. Mfold Web Server for Nucleic Acid Folding and Hybridization Prediction. *Nucleic Acids Res.* **2003**, *31*, 3406–3415.
- Do, C. B.; Woods, D. A.; Batzoglou, S. Contrafold: RNA Secondary Structure Prediction without Physics-Based Models. *Bioinformatics* **2006**, *22*, e90–98.
- Bindewald, E.; Shapiro, B. A. RNA Secondary Structure Prediction from Sequence Alignments Using a Network of K-Nearest Neighbor Classifiers. *RNA* **2006**, *12*, 342–352.
- Knudsen, B.; Hein, J. Pfold: RNA Secondary Structure Prediction Using Stochastic Context-Free Grammars. *Nucleic Acids Res.* **2003**, *31*, 3423–3428.
- Bernhart, S. H.; Tafer, H.; Muckstein, U.; Flamm, C.; Stadler, P. F.; Hofacker, I. L. Partition Function and Base Pairing Probabilities of RNA Heterodimers. *Algorithms Mol. Biol.* **2006**, *1*, 3.
- Andronescu, M.; Zhang, Z. C.; Condon, A. Secondary Structure Prediction of Interacting RNA Molecules. *J. Mol. Biol.* **2005**, *345*, 987–1001.
- Zadeh, J. N.; Wolfe, B. R.; Pierce, N. A. Nucleic Acid Sequence Design Via Efficient Ensemble Defect Optimization. *J. Comput. Chem.* **2010**, *32*, 439–452.
- Aguirre-Hernandez, R.; Hoos, H. H.; Condon, A. Computational RNA Secondary Structure Design: Empirical Complexity and Improved Methods. *BMC Bioinf.* **2007**, *8*, 34.
- Andronescu, M.; Fejes, A. P.; Hutter, F.; Hoos, H. H.; Condon, A. A New Algorithm for RNA Secondary Structure Design. *J. Mol. Biol.* **2004**, *336*, 607–624.
- Busch, A.; Backofen, R. Info-RNA—a Server for Fast Inverse RNA Folding Satisfying Sequence Constraints. *Nucleic Acids Res.* **2007**, *35*, W310–313.
- Busch, A.; Backofen, R. Info-RNA—a Fast Approach to Inverse RNA Folding. *Bioinformatics* **2006**, *22*, 1823–1831.
- Dirks, R. M.; Lin, M.; Winfree, E.; Pierce, N. A. Paradigms for Computational Nucleic Acid Design. *Nucleic Acids Res.* **2004**, *32*, 1392–1403.
- Bindewald, E.; Hayes, R.; Yingling, Y. G.; Kasprzak, W.; Shapiro, B. A. RNAjunction: A Database of RNA Junctions and Kissing Loops for Three-Dimensional Structural Analysis and Nanodesign. *Nucleic Acids Res.* **2008**, *36*, D392–397.
- Bindewald, E.; Grunewald, C.; Boyle, B.; O'Connor, M.; Shapiro, B. A. Computational Strategies for the Automated Design of RNA Nanoscale Structures from Building Blocks Using Nanotiler. *J. Mol. Graphics Modell.* **2008**, *27*, 299–308.
- Seiffert, J.; Huhle, A. A Full-Automatic Sequence Design Algorithm for Branched DNA Structures. *J. Biomol. Struct. Dyn.* **2008**, *25*, 453–466.
- Seeman, N. C. Nucleic Acid Junctions and Lattices. *J. Theor. Biol.* **1982**, *99*, 237–247.
- Wenzel, W.; Hamacher, K. Stochastic Tunneling Approach for Global Minimization of Complex Potential Energy Landscapes. *Phys. Rev. Lett.* **1999**, *82*, 3003–3007.
- Baldi, P.; Brunak, S.; Chauvin, Y.; Andersen, C. A.; Nielsen, H. Assessing the Accuracy of Prediction Algorithms for Classification: An Overview. *Bioinformatics* **2000**, *16*, 412–424.
- Afonin, K. A.; Danilov, E. O.; Novikova, I. V.; Leontis, N. B. TokenRNA: A New Type of Sequence-Specific, Label-Free Fluorescent Biosensor for Folded RNA Molecules. *ChemBiochem* **2008**, *9*, 1902–1905.

42. Afonin, K. A.; Leontis, N. B. Generating New Specific RNA Interaction Interfaces Using C-Loops. *J. Am. Chem. Soc.* **2006**, *128*, 16131–16137.
43. Kasprzak, W.; Bindewald, E.; Kim, T. J.; Jaeger, L.; Shapiro, B. A. Use of RNA Structure Flexibility Data in Nanostructure Modeling. *Methods* **2011**, *54*, 239–250.
44. Torelli, A. T.; Krucinska, J.; Wedekind, J. E. A Comparison of Vanadate to a 2'-5' Linkage at the Active Site of a Small Ribozyme Suggests a Role for Water in Transition-State Stabilization. *RNA* **2007**, *13*, 1052–1070.